

# Investigation of the Formation of Physical Damage on Automotive Finishes Due to Acidic Reagent Exposure

D. F. WHITE, R. E. FORNES,\* R. D. GILBERT, and J. A. SPEER

North Carolina State University, Box 8202, Raleigh, North Carolina 27695-8202

## SYNOPSIS

Automotive paints with clear-coat surfaces can be physically damaged by exposure to acidic reagents produced in a smog chamber designed to reproduce real environmental conditions. Visual and reflectance microscopy observations show that deposition of material formed from the reaction of the clear coat and the reagent drop occurs on the paint surface after the drop evaporates to a critical size, with the greatest deposition occurring at the edge of the drop. This type of deposition suggests a free-energy minimization process favoring the formation of stable nuclei at the reagent drop edge. With heating after the drop evaporation to simulate exposure to the sun, a damaged area containing sulfur that is in the shape of a circular ring is observed at the location of the deposits. The majority of the visual damage appears to result from an interaction between the deposit and the paint at elevated temperatures. Results from profilometry, scanning electron microscopy, and reflectance microscopy show that the damaged areas are ring-shaped cracked blisters on the surface resulting from the clear coat separating into layers. © 1993 John Wiley & Sons, Inc.

## INTRODUCTION

Damage to automobile finishes due to acidic precipitation has been observed over the past several years.<sup>1</sup> This damage is typically in the form of circular or irregular areas that appear to be deposits to the naked eye that cannot be removed by washing. White and Rothschild observed spotting and sometimes pitting on the surfaces of field-exposed automobiles in Israel that they linked to acid rain.<sup>2</sup> This problem is of concern to U.S. automotive manufacturers.<sup>3</sup> Newer automotive paint formulations contain unpigmented clear coats,<sup>3</sup> and this study tests the susceptibility to acidic pollutants of several clear-coated systems.

Here, a model of the damage process caused by acidic reagents that closely resemble environmentally produced precipitation is proposed. These reagents were produced in a smog chamber located at North Carolina State University (NCSU) designed to reproduce real environmental conditions. In ad-

dition, methods to observe and monitor the damage to automotive paints caused by acidic reagents are reported.

## EXPERIMENTAL

Three clear-coat paints having an hydroxyl-containing acrylic resin were studied. Paint #1 was cross-linked with diisocyanates. Paint #2 was cross-linked with diisocyanates and melamine formaldehyde, and paint #3 was cross-linked with melamine formaldehyde. The base coat of all three paints was an hydroxyl-containing acrylic resin cross-linked with melamine formaldehyde.

The paint samples were exposed to three different dewes formed in an environmental smog chamber at NCSU.<sup>4</sup> This chamber is essentially a stirred tank reactor into which measured amounts of sulfur dioxide, nitric oxide, propylene, purified air, and water are injected under the influence of UV light. In this environment, an artificial smog forms consisting of SO<sub>2</sub>, NO<sub>x</sub>, O<sub>3</sub>, PAN, H<sub>2</sub>O, H<sub>2</sub>SO<sub>4</sub>, HNO<sub>3</sub>, HCOOH, and CH<sub>3</sub>COOH. The pollutants, air, and water are continuously injected into the chamber to

\* To whom correspondence should be addressed.

**Table I** Anion and Cation Concentration Levels ( $\mu\text{mol/L}$ )

Chamber Dew	pH	$\text{SO}_4^{2-}$	$\text{NO}_3^-$	$\text{Cl}^-$	$\text{Ca}^{2+}$	$\text{Mg}^{2+}$	$\text{Na}^+$	$\text{K}^+$
A	4.1	119	112	77	20	10	30	20
B	4.2	101	55	33	0	0	0	0
C	3.5	334	27	40	0	0	0	10

maintain the smog composition. After the reactor reaches steady-state conditions, the smog is circulated through channels where dew forms on chilled stainless-steel plates coated with Teflon. In these experiments, the resulting condensate was collected in high-density polyethylene containers and aliquots were taken for ion chromatographic analyses.

A partial list of the anions and cations in the dews, their concentrations, and pH at the time of use is given in Table I. The paints were also exposed

to pH 4 sulfuric/nitric acid (mixed 50/50 by volume).

Anion concentrations in the dews were determined with a Dionex Model 10 ion chromatograph modified by the addition of pulse dampers, high-pressure valves, an electropneumatic valve control, an eluent degas and delivery system, a regenerate delivery system, and a pulse amperometric detector. Concentrations of the cations were determined using a Perkin-Elmer 5000 atomic absorption spectro-

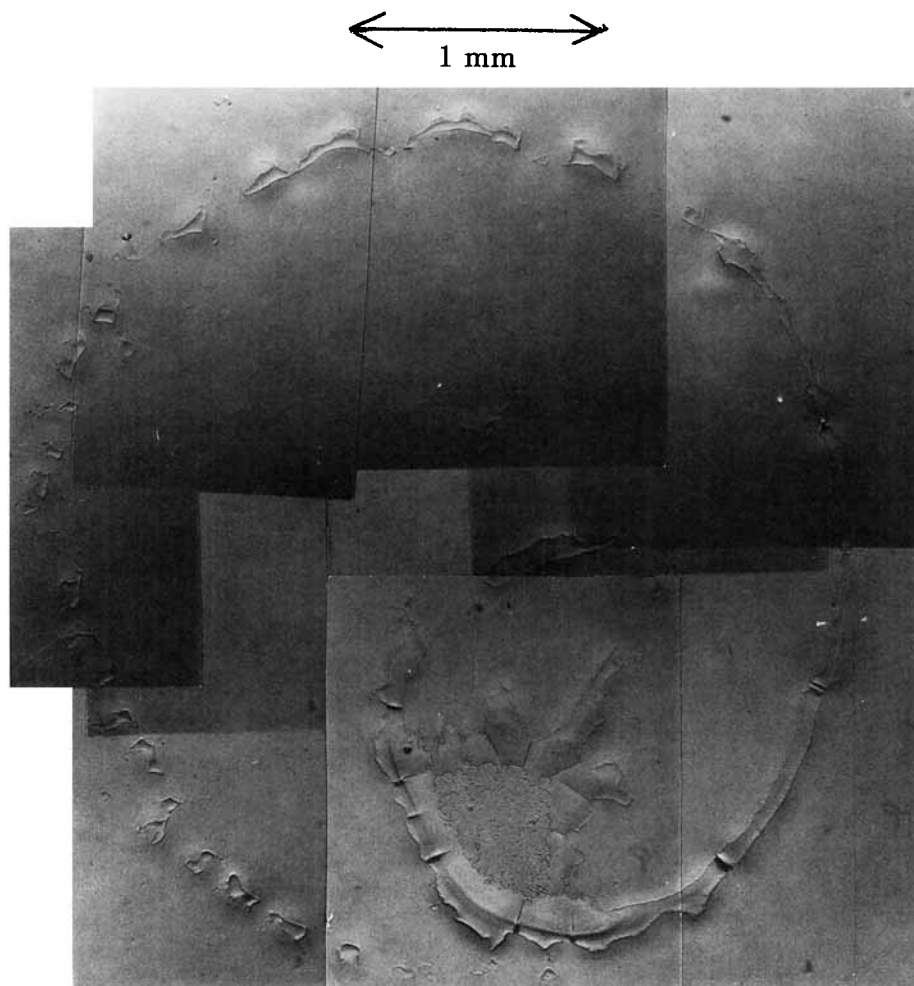


**Figure 1** Chamber dew C damage—paint #3: 1 h room temperature exposure ( $60 \mu\text{L}$  drop) followed by 24 h at  $70^\circ\text{C}$ .

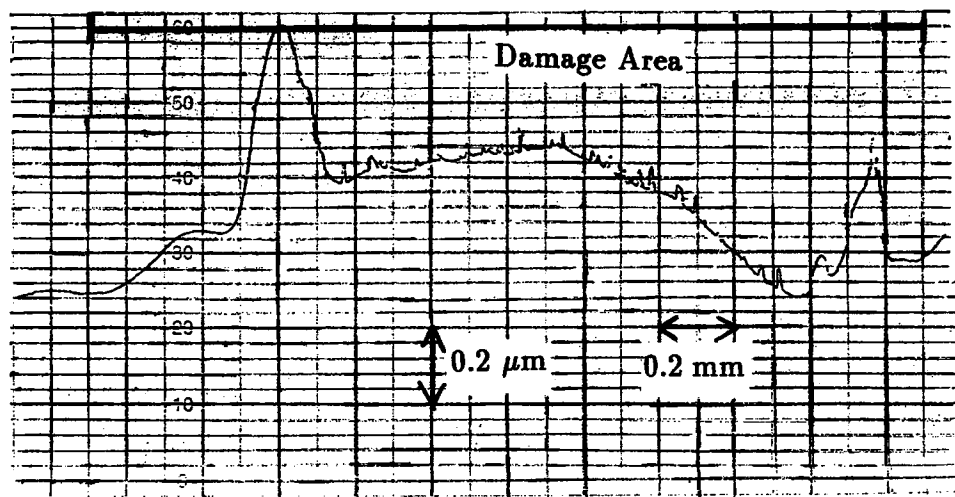


**Figure 2** Profile of chamber dew C damage—Paint #1: 50 min. exposure (30  $\mu\text{L}$  drop) at 54°C; 50,000  $\times$  vertical magnification.

photometer. Both techniques are methods of choice for determination of the ions analyzed according to the U.S. Environmental Protection Agency.<sup>5,6</sup> Values of pH were determined using a Fisher Scientific Accumet pH meter Model 900.

Before exposure, the paint sample surfaces were rinsed with deionized water and buffed with a chamois to remove any contaminations. Then, three drops of equal volume of each type of reagent were pipetted onto the sample surfaces equal distances apart. The samples were then heated either in an oven or on a hotplate to temperatures exceeding 50°C. After exposure, the plates were allowed to cool, rinsed with water, and buffed with a chamois.

Reflectance microscopy observations of the sample surfaces were performed using a Nikon Optiphot-Pol polarizing light microscope equipped with a Nikon CFW 10XCM eyepiece and a Nikon CF M plan objective. Photomicrographs were obtained using a Microflex Model AFX-IIA camera attachment. Surface profiles and quantitative surface shape information were obtained using a Talystep profilometer (Rank Taylor Hobson). Elemental mappings of the damaged areas were produced using an Amray 1000 SEM in combination with a Princeton Gamma-Tech Eimix imaging system and a PGT model LS-15 electron dispersive spectroscopy detector.

## RESULTS AND DISCUSSION

A drop exposure test was used to simulate the beading that occurs on horizontal automobile paint surfaces after rain or dew exposure. This type of test

also enables comparisons with adjacent areas of the paint that were unexposed. Exposure temperatures of greater than 50°C were used to model the process of outdoor exposure of automobile paints at their maximum temperature of exposure that can commonly exceed 90°C due to heating from sunlight.<sup>1</sup> One test was performed for 26 h at 20°C, but no visual damage was detected.

All the chamber dews created ring-shaped, fractured blisters on the clear-coat surfaces upon heating to temperatures exceeding 50°C (Fig. 1). Microscopy observations confirmed that the clear coat had also separated into layers. The ring form of the damage suggests a free-energy minimization process favoring concentration of the damaging reagent at

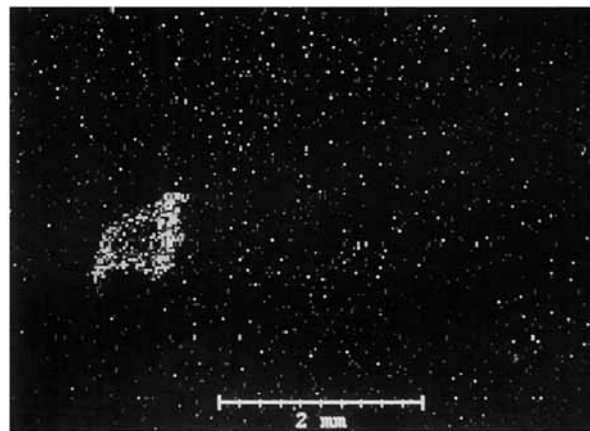


**Figure 3** Chamber dew C damage, sulfur mapping—paint #3: 1 h room temperature exposure (60  $\mu\text{L}$  drop) followed by 24 h at 70°C.

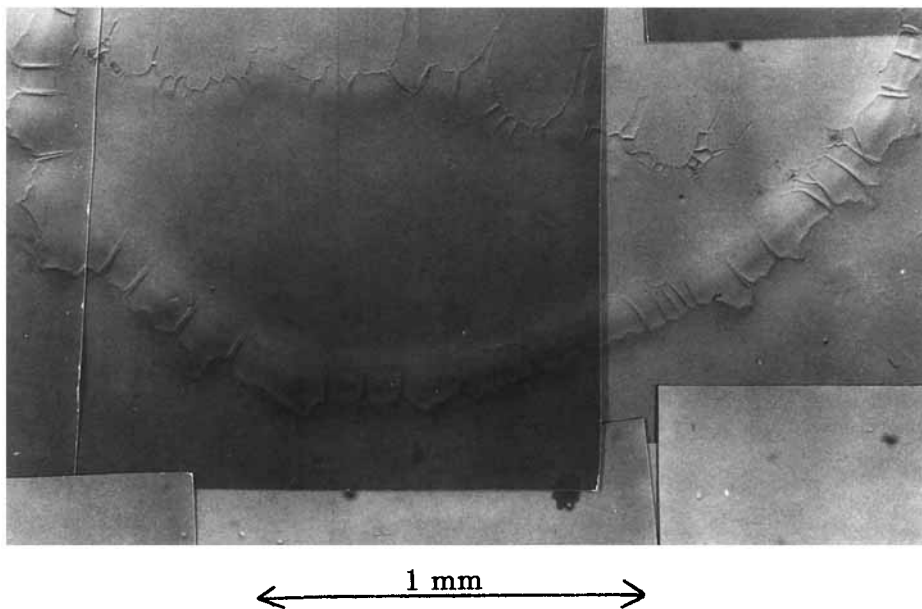


**Figure 4** Chamber dew B damage—paint #2: 1 h room temperature exposure (60  $\mu$ L drop) followed by 24 h at 70°C.

the edge of the evaporating drop (as discussed below). With profilometry, the rings are easily detected. In the example in Figure 2, the blister height (left side) is approximately 0.6  $\mu$ m above the level

surface of the paint. Blistering is also noticeable inside the blister ring.

Figure 3 is an X-ray compositional sulfur mapping of the same damage area shown in Figure 1. The

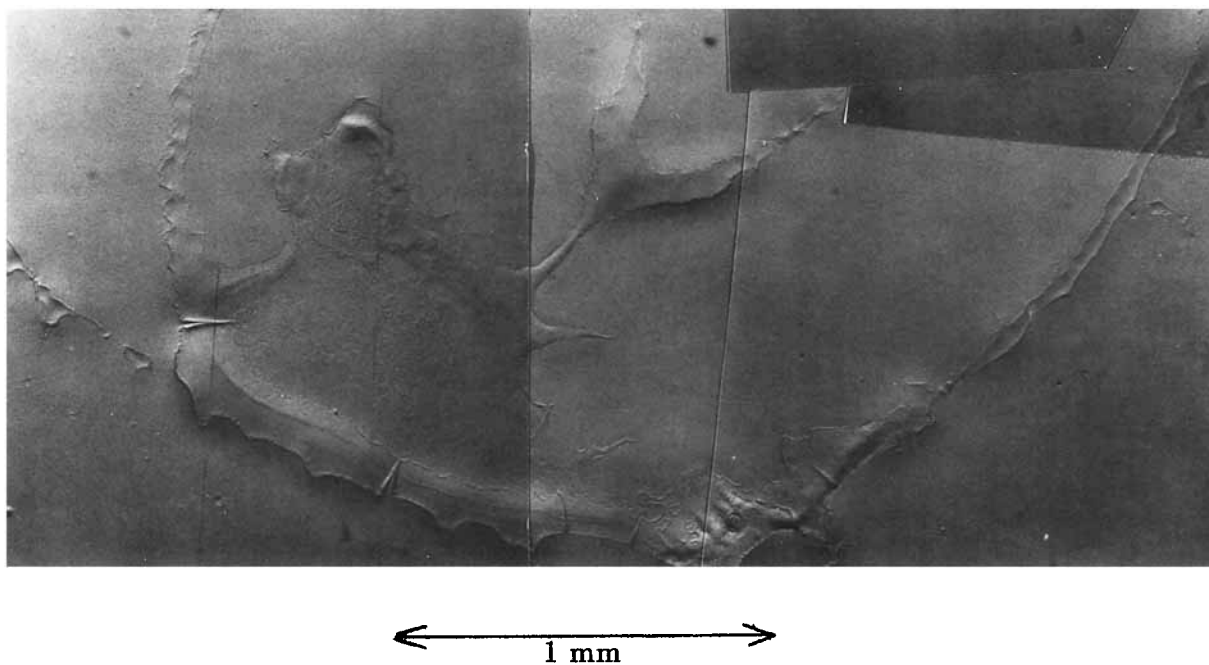


**Figure 5** Chamber dew C damage—paint #2: 1 h room temperature exposure (60  $\mu$ L drop) followed by 24 h at 70°C.

lighter the tone on the map, the higher the concentration of sulfur in that particular part of the damage area. Most of the sulfur is located in the area that had the heaviest damage (the other bright areas are background levels). The samples were rinsed and buffed after exposure, suggesting that the sulfur had chemically combined with the paint in a form resistant to buffing.

Portions of the most damaged areas created by drops of chamber dews B and C and pH 4 sulfuric/nitric acid (mixed 50/50 by volume) are shown in Figures 4–6. Ring-shaped damage is again evident. Chamber dew C caused slightly more damage than did chamber dew B, which is probably a result of dew C having a lower pH than that of dew B (pH 3.5 vs. pH 4.2). Chamber dew B (pH 4.2) caused much more damage than did the sulfuric/nitric acid mixture (pH 4.0), indicating that the damage level is not a function of pH alone, but that the chemistry of the dews plays an important role in the degradation.

#### Effects of Chamber Dew Deposits, Time of Exposure, and Temperature

Visual observations of samples with dew drops, while being heated at 70°C, showed that material is deposited on the paint surface from the chamber dew drops as they evaporate. After the drops evaporated

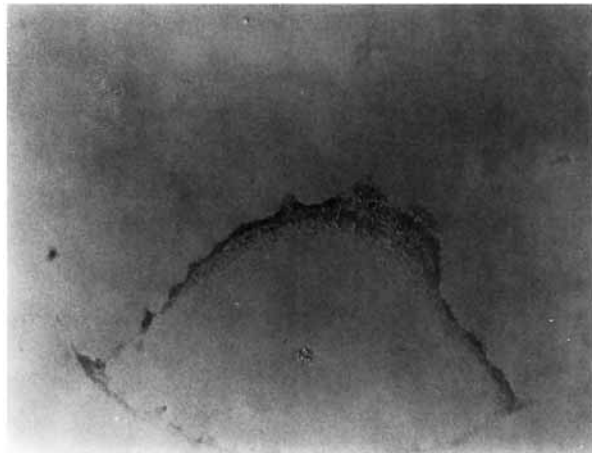


**Figure 6** pH 4 sulfuric/nitric acid damage—paint #2: 1 h room temperature exposure (60  $\mu$ L drop) followed by 24 h at 70°C.

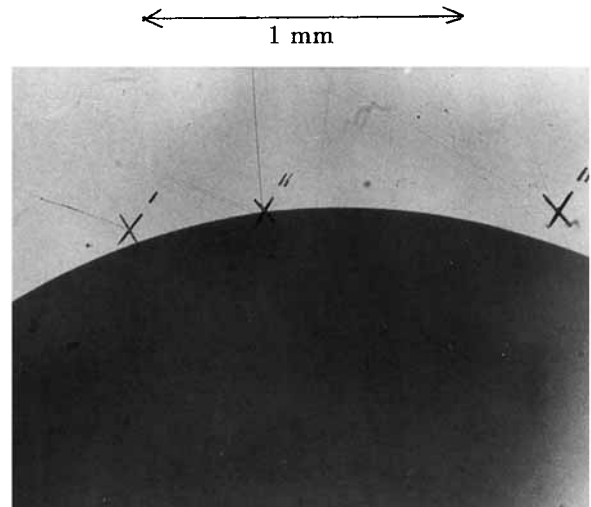


**Figure 7** Chamber dew A (5  $\mu$ L drop) on paint #3 surface: 0 min at 30°C. (X's indicate reference points on surface of paint.)

and the paint surface had been rinsed and buffed, low-level damage in the form of a circular ring was observed and it was located at the same place on the surface where deposits had formed. With continued heating, no further damage occurred. If, however, the deposits were left on the surface and heating continued for up to 24 h, final damage levels were greater, with the levels of damage increasing with longer heating times. These results are similar to those of Wolff et al. where they observed that car paints exposed to one wetting event of natural precipitation continued to degrade after exposure to ambient temperature and sunlight, but when the surfaces were washed, no further damage occurred.<sup>1</sup>

It appears that the majority of the visual damage results from an interaction between the deposit and the paint and is not due to a reaction between the dew and the paint. Higher temperatures (at least up to 90°C) and longer heating times (at least up to 24 h) result in more severe damage.

#### Observations of Chamber Dew Evaporation on Paint Surface

Reflectance microscopy observations of the evaporation of chamber dews on the paint surfaces show that little change of the clear-coat surface of the paints occurs until a critical drop size is reached. Figures 7–12 show the drop size at various times during the evaporation process. Initially, only evaporation of the dew occurs. The dark circular area in each photomicrograph is the evaporating drop observed directly above the drop, and the paint surface

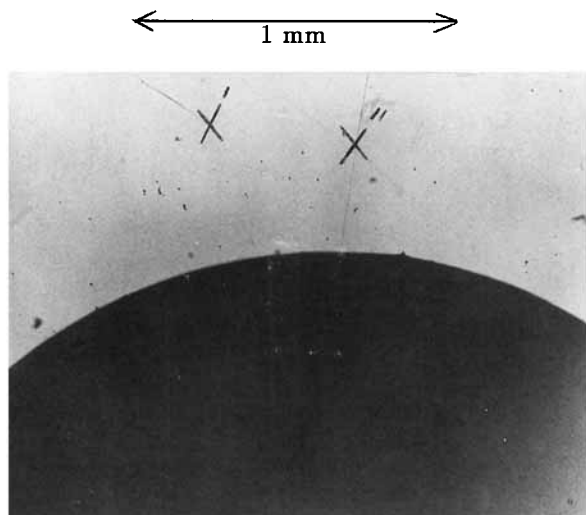


**Figure 8** Chamber dew A on paint #3 surface: 2 min at 30°C. (X's indicate reference points on surface of paint.)

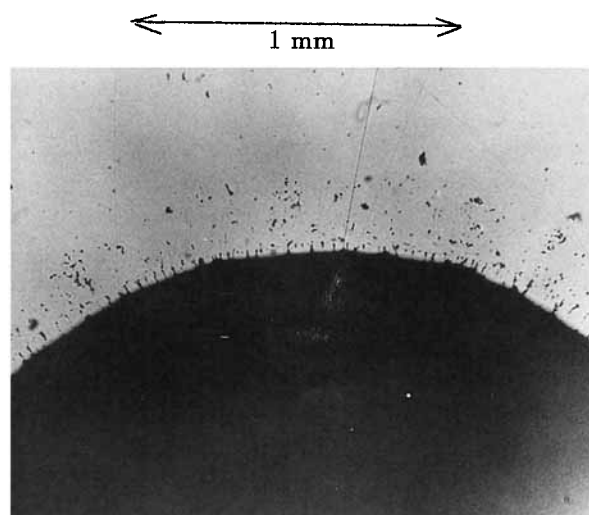


**Figure 10** Chamber dew A on paint #3 surface: 6 min at 30°C. (X's indicate reference points on surface of paint.)

can be seen as the light area. The X's are reference points on the paint surface at the initial edge of the drop. Near the critical concentration, the drop diameter decreases more slowly and precipitation levels increase (Figs. 10 and 11). When the drop reaches a critical diameter, it remains fairly constant, while a large amount of precipitate material forms at the outer edge of the drop, forming a ring of deposits. At this point in the evaporation process, the contact angle between the surface of the paint and the drop decreases, resulting in a flattening of the drop surface. Finally, at a certain volume level, the surface of the drop collapses, leaving deposits

inside the initial ring, and the drop remaining quickly evaporates. Figures 12 and 13 show the collapse in progress and the precipitate material left on the paint surface immediately after the evaporation of the entire drop. The damage on the paint surface produced after 2 h of heating at 85°C is shown in Figure 14 after washing and buffing. The nature of the damage is similar to that produced by all the chamber dews, with highest levels being generally located in a ring or in the approximate center of the damage area.

Figure 15 is a photomicrograph of a chamber dew drop on a glass slide. The somewhat irregular shape

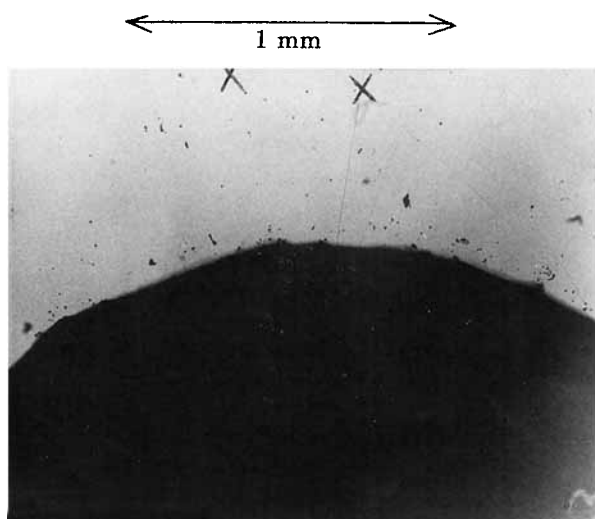


**Figure 9** Chamber dew A on paint #3 surface: 4 min at 30°C. (X's indicate reference points on surface of paint.)

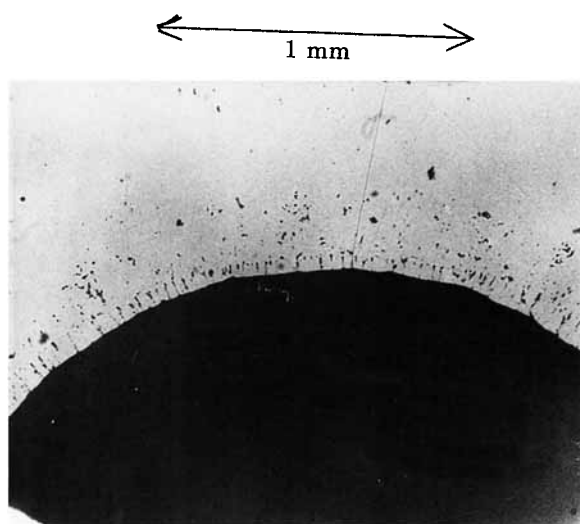


**Figure 11** Chamber dew A on paint #3 surface: 8 min at 30°C. (X's indicate reference points on surface of paint.)

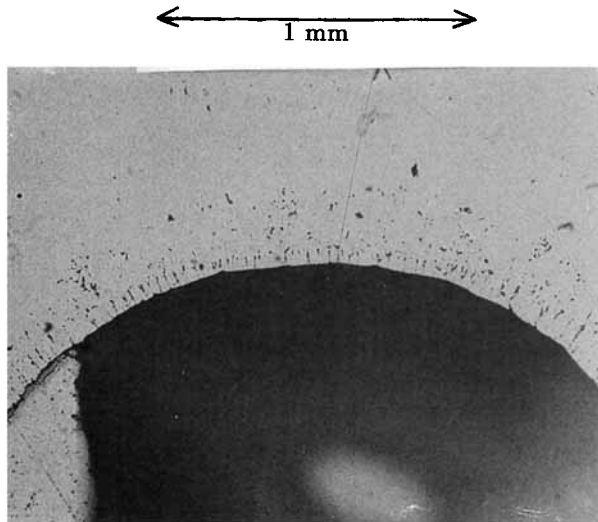


**Figure 12** Collapse of dew A drop surface on paint #3: 10 min at 30°C. (X's indicate reference points on surface of paint.)

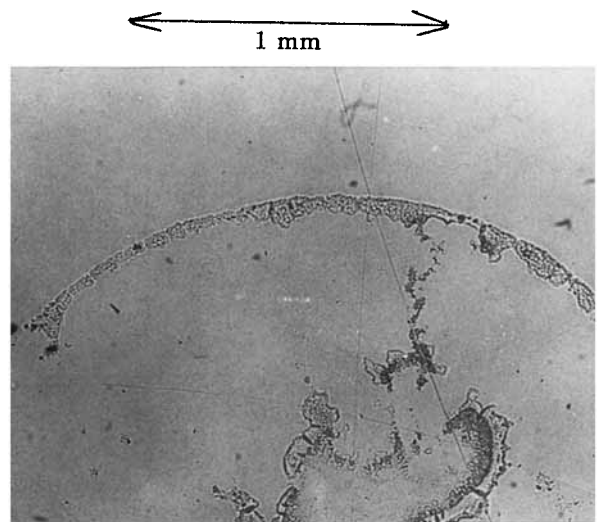


**Figure 14** Damage produced by chamber dew A on paint #3: 11 min at 30°C + 2 h at 85°C. (Sample was washed and buffed.)

of the drop is due to the poor wetting of the glass. After complete evaporation of the dew drop at 85°C (about 5 min), the deposits shown in Figure 16 remain. There is little deposition on the glass slide compared to the paints (compare Fig. 16 with Fig. 13). The precipitate observed on the glass slide may be the nonvolatile component of the chamber dew. After washing with deionized water and a single buffing, a small amount of surface deposits can be observed (Fig. 17). Glass is relatively unreactive with the acids that compose the majority of the composition of the dew, and so little precipitation

occurs in contrast to the deposits formed on the paint. Since there is only a small deposit formed on the glass, we therefore conclude that the most likely source of the deposit on the paint is from a chemical reaction between the paint and the dew.

**Model of Physical Damage Formation**

As shown above, the largest amounts of residual material are deposited at the edge of the evaporating drop. This location appears to be the most favorable for the creation of nucleating centers to initiate precipitation. Favorable locations for nucleation in solutions are at the surface of solutions (the drop sur-

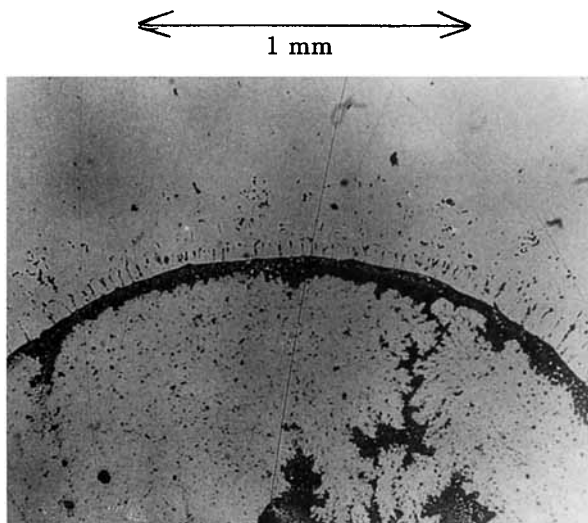


**Figure 13** Dew A deposit on paint #3 surface: 11 min at 30°C. (X's indicate reference points on surface of paint.)

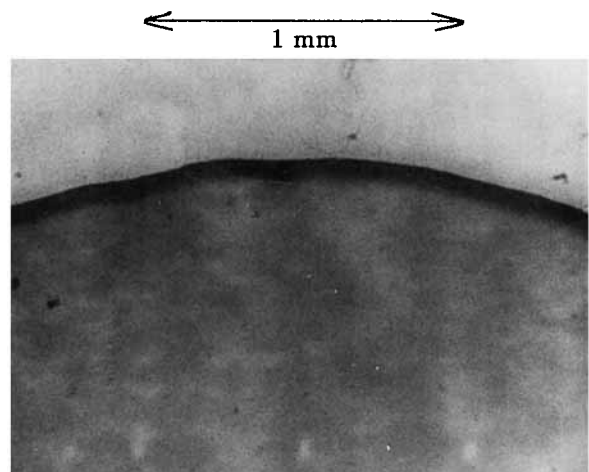


**Figure 15** Chamber dew (5 µL drop) on glass slide.



face in our case) or on the walls of the vessel containing the solution (the drop-paint interface in our case), because the free energy of formation of a nucleating center is reduced at these locations.<sup>7</sup>

Excluding the strain and configurational entropy terms that can be neglected to first approximation, the free energy of formation ( $\Delta G$ ) of a nucleating center can be written

$$\Delta G \sim V\Delta G_v + \sum_{i=1} A_i\sigma_i$$

where  $V$  is the volume of the nucleating center;  $\Delta G_v$ , the difference in the Gibbs free energy per unit volume between the solid and liquid phases; and  $A_i$  and  $\sigma_i$ , the surface area and interfacial free energy of the  $i$ th facet, respectively.<sup>8</sup> For the surfaces  $A_i$  lying along the drop surface or the drop-paint interface, the interfacial free energy  $\sigma_i$  is lower than the interfacial free energy of a surface located inside the drop.<sup>7</sup> A nucleating center at the edge of the drop has surfaces in contact with two favorable locations (drop surface and drop-paint interface) simultaneously, resulting in a further decrease in the free energy of formation. Since the free energy of formation is lowest at the edge of the drop, the critical size of a nucleating center necessary to begin precipitation is reduced compared to other locations, with the result that the nucleation rate is largest at the edge of the drop.<sup>9</sup> As a result, the largest precipitate levels occur at the drop edge.

This is in agreement with experimental studies of nucleation and crystallization in the soda-lime-silica system by Strnad and Douglas.<sup>10</sup> They found

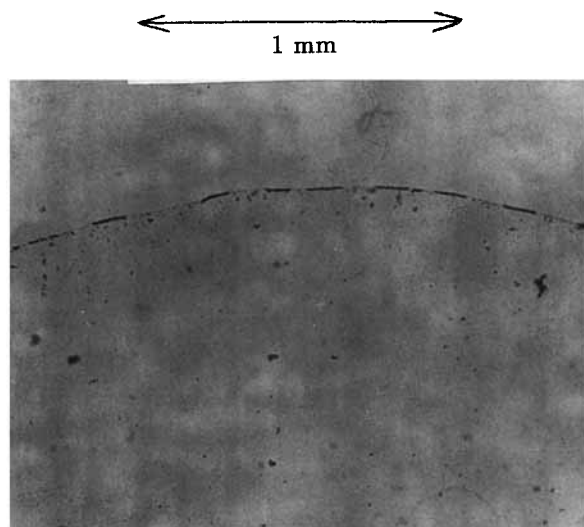


**Figure 16** Chamber dew A deposit on glass slide.

← 1 mm →

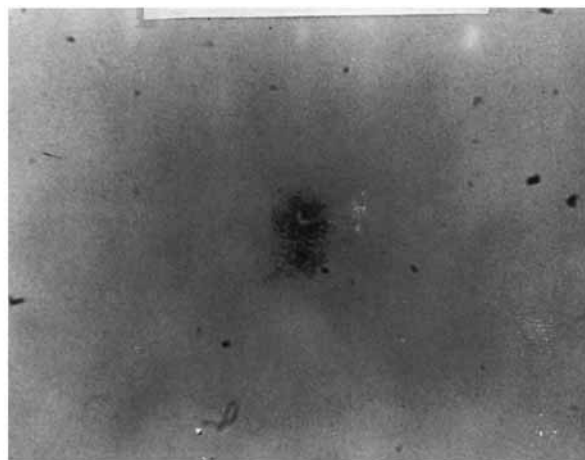


**Figure 17** Damage produced by chamber dew A on glass slide: 6 min at 85°C + washing and buffing.

surface nucleation to occur more readily than homogeneous nucleation at the same degree of cooling, with many more crystals nucleating on 1 cm<sup>2</sup> of surface than within 1 cm<sup>3</sup> of volume. They suggest that this implies that there is a mechanism that reduces the amount of energy needed to form a nucleus below that normally required by considerations of surface energy between a homogeneous nucleus and the parent liquid. Burnett and Douglas showed that nucleation occurs preferentially on surfaces, especially when they are scratched.<sup>11</sup> Nucleation can also proceed more easily on surfaces when there is contamination, since the nucleation rate is enhanced in the presence of foreign particles such as dust that often contaminate surfaces.<sup>12</sup>

## CONCLUSIONS

Results from these investigations indicate that aqueous solutions of composition and pH comparable to natural precipitation cause considerable damage to automotive coatings. The chamber dews produced deposits on the coating surfaces as a result of a reaction between the dews and the clear coats. After heating, ring-shaped fractured blisters containing sulfur formed on the clear-coat surface in the areas on the paint surface that had been exposed to chamber dews, with the clear coat separating into layers. Visual damage on the paint surface appeared to occur as a result of a reaction between the deposited material and the clear coat, with the damage levels on the surface increasing as the time of heating



increased. The ring form of the damage resulted from the deposits forming in a ring shape. This shape appeared to be a result of a nucleation process that favored formation of deposits at the edge of the evaporating drop. The edge is the most favorable location because the free energy of formation of a nucleating center is lowest at the drop edge.

The authors would like to thank John Spence and Tom Lemmons of the U.S. EPA for providing the SEM photograph.

## REFERENCES

1. G. T. Wolff, W. R. Rodgers, D. C. Collins, M. H. Verma, and C. A. Wong, *J. Air Waste Management Assoc.*, **40**, 1638 (1990).
2. J. White and W. Rothschild, *Metal Finish.*, **85**(5), 15 (1987).
3. T. C. Simpson and P. J. Moran, *National Acid Precipitation Assessment Program State-of-Science/Technology Report 19*, May 1990.
4. J. W. Spence, E. O. Edney, F. H. Haynie, D. C. Stiles, E. W. Corse, M. S. Wheeler, and S. F. Cheek, in *Corrosion Testing and Evaluation: Silver Anniversary Volume*, ASTM STP1000, R. Baboian and S. W. Dean, Eds., Am. Soc. Test. Mat., Philadelphia, 1990.
5. U. S. Environmental Protection Agency, EPA600/4-82-042a+b, March 1983.
6. U. S. Environmental Protection Agency, EPA600/4-79-020, March 1983.
7. D. Elwell and H. J. Scheel, *Crystal Growth from High-Temperature Solutions*, Academic Press, London, 1975.
8. A. G. Walton, in *Nucleation*, A. C. Zettlemoyer, Ed. Marcel Dekker, New York, 1969, p. 225.
9. R. J. Kirkpatrick, in *Kinetics of Geochemical Processes*, Reviews in Mineralogy, Vol. 8, A. C. Lasaga and R. J. Kirkpatrick, Eds., Min. Soc. Am., Washington, DC, 1981.
10. Z. Strnad and R. W. Douglas, *Phys. Chem. Glass.*, **14**, 33 (1973).
11. D. G. Burnett and R. W. Douglas, *Phys. Chem. Glass.*, **12**, 117 (1971).
12. A. A. Chernov, *Modern Crystallography III—Crystal Growth*, Springer Series in Solid State Sciences, Vol. 36, Hans-Joachim Quaisser, Ed., Springer-Verlag, Berlin, 1984.

Received October 8, 1992

Accepted February 19, 1993